Characterization of platinum and titanium thermistors for terahertz antenna-coupled bolometer applications

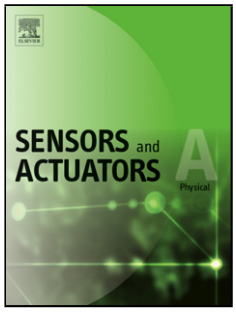

Title: Characterization of Platinum and Titanium Thermistors for Terahertz Antenna-Coupled Bolometer Applications

Authors: Amit Banerjee, Hiroaki Satoh, Yash Sharma, Norihisa Hiromoto, Hiroshi Inokawa

PII: S0924-4247(17)31751-X
DOI: https://doi.org/10.1016/j.sna.2018.02.014
Reference: SNA 10636

To appear in: *Sensors and Actuators A*

Received date: 28-9-2017
Revised date: 13-1-2018
Accepted date: 8-2-2018

Please cite this article as: Banerjee A, Satoh H, Sharma Y, Hiromoto N, Inokawa H, Characterization of Platinum and Titanium Thermistors for Terahertz Antenna-Coupled Bolometer Applications, *Sensors and Actuators: A Physical* (2010), https://doi.org/10.1016/j.sna.2018.02.014

Characterization of Platinum and Titanium Thermistors for Terahertz Antenna-Coupled Bolometer Applications

Amit Banerjee[1], Hiroaki Satoh[1], Yash Sharma[2],

Norihisa Hiromoto[2], and Hiroshi Inokawa[1*]

[1]Research Institute of Electronics, Shizuoka University,
[2]Graduate School of Science and Technology, Shizuoka University, 3-5-1 Johoku, Naka-ku, Hamamatsu 432-8011, Japan

Author to whom correspondence should be addressed.
*Electronic mail: *inokawa.hiroshi@shizuoka.ac.jp*, Phone no. +81-53-478-1308

Graphical abstract

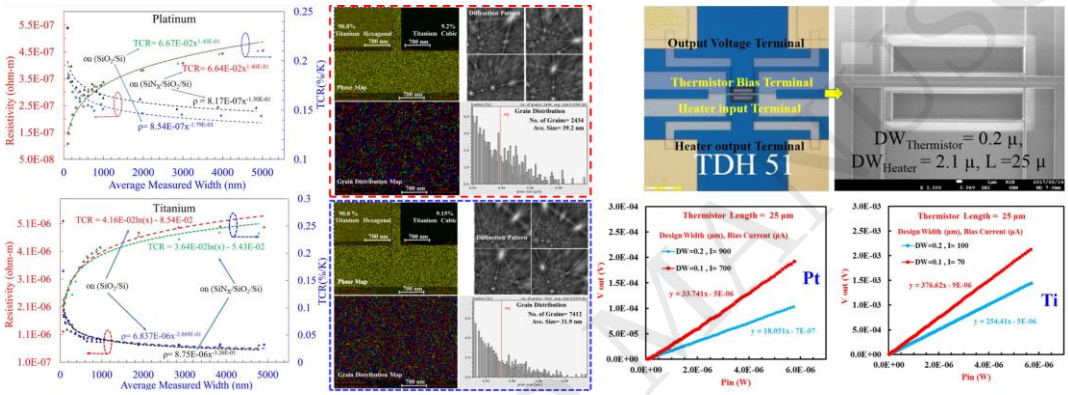

Highlights

- Microbolometer is a radiation detector for infrared (IR) and terahertz (THz) waves
- Responsivity is proportional to temperature coefficient of resistance of thermistor
- Narrow-width effects on TCR and resistivity of Pt & Ti thermistor are investigated
- Device with Ti thermistor has higher responsivity than with Pt thermistor
- Device with Ti thermistor width of 0.1 µm has higher responsivity than width 0.2 µm

Abstract:

Microbolometer is a radiation detector for infrared (IR) and terahertz (THz) waves. The temperature coefficient of resistance (TCR) of the thermistor is a vital factor, as the responsivity is proportional and noise equivalent power (NEP) is inversely proportional to it. The narrow-width effect on TCR and resistivity on two different substrates (SiO_2/Si and SiN_X/SiO_2/Si) for platinum (Pt) and titanium (Ti) thermistor with various design width (DW)= 0.1~5 µm are investigated. Increased resistivity and reduced TCR of the devices with the decreased line width, is observed commonly for both metal and fitted with

empirical formulae, which hold well for different substrates. It is evident from electron backscatter diffraction (EBSD) results showing reduced average grain size form Ti film to Ti nanowire (DW=0.1 µm), that the reduced TCR is not dependent on crystal orientation or phase variation of material but can be correlated with reduced grain size due to reduction of width. The optimum value considering design requirement, thermistor of DW =0.1 µm and 0.2 µm is used further for the fabrication of microbolometers. It is found that the device with DW= 0.1 µm of Ti thermistor has ~ 1.5 times higher electrical responsivity (376 V/W) at maximum allowable current than that with DW= 0.2 µm (254 V/W), which is also ~11 times higher than device with DW= 0.1 µm of Pt thermistor.

Keywords: Terahertz detector, Microbolometer, Narrow-width effect, Metal thermistor, Responsivity.

1. Introduction

Enormous emphasize has been given to the modern thermal detector technology due to the increased demand in imaging for surveillance, security inspection, equipment maintenance, etc. Terahertz (THz) technology which deals with the thermal radiation in the region from 300 GHz to 3 THz (wavelength from 100 µm to 1 mm) has drawn attention with exciting possibilities in past decade due to the advancement of related semiconductor material science and nanoscale fabrication technologies [1]. Electromagnetic wave around 1 THz comes with attractive features for non-contact and non-invasive sensing and yields high-resolution images compared to millimeter or longer waves. These are nonionizing and not harmful for low photon energies, and may be used on live tissues. Other applications of THz waves include: ultrahigh-speed wireless communications, biomedical screening and diagnosis, drug discovery, and environmental and food analysis, surveillance, radio telescopes, spectral analysis of interstellar medium and planetary atmospheres [2-9]. However, the present-day capacity of THz technology is quiet insufficient in terms of sensitivity and speed of measurements, and farther research on the sources, detectors and sensing systems are vital for extending the operations of THz waves in actual applications.

Unlike photon detectors, thermal detectors, represented by a microbolometer, do not need additional cryogenic support [10]. However, current uncooled microbolometers performance in terms of detectivity and response time suffers because of high thermal noise, self-heating under constant bias [11,12] and vulnerability of the sensor material [13]. Structurally, microbolometers include an absorber that receives the electromagnetic radiation and transfers the energy to the thermistor. For longer wavelength in THz domain, the large absorbers can no longer be sustained structurally and with proper thermal isolation, as an antenna-coupled microbolometer becomes more feasible [14-16]. It is also crucial to optimize the thermistor and the heater independently with electrical separation but thermal combination for achieving higher sensitivity [15]. Another important aspect shown by our electromagnetic simulation is the load matching between the heater and antenna for maximum power transfer [16]. However other than these

design aspects, the performance of the detector is also susceptible to the materials properties of the resistive element, i.e. thermistor. The consideration of temperature coefficient of resistance (TCR) of the thermistor material is extremely crucial as the responsivity (ratio of output voltage to input power), is proportional to the TCR and also the noise equivalent power (NEP, minimum detectable power of the receiving signal) is inversely proportional to the TCR. In materials aspect, using metallic thermistors like platinum (Pt) or titanium (Ti) is advantageous due to the low noise, which is mainly the shot and thermal noises, and hence device performance directly depends on the improved (higher) TCR, which is not the case with high-TCR materials like VO_x and a-Si. Pt has been historically used as a temperature sensor, due to its immunity to oxidation or chemical reaction and hence stability. Also Ti is selected as possible thermistor candidate along with heater material considering it has low thermal and electrical conductivities, and is immune to electromigration [17-19]. A higher resistivity of the thermistor material is also useful. However, this may face a trade-off with TCR, and may not always be desirable. Hence, another feature may be the length of thermistor, which could be availed by more complex layout pattern of the thermistor, e.g. meander shape, with longer effective length, resulting in enhanced electrical responsivity [19,20].

Importantly, as metal conductors (Pt, Ti, etc.) approaches the dimensions comparable to the mean free path of the conduction electrons, size effects may impose limitations on the ultimate electrical properties achievable by the metal interconnects, which has been serious concern for the ultralarge-scale integration (ULSI). The current microbolometer fabrication encounters performance issues due to the utilized narrow (0.1 or 0.2-μm-wide) metal line having a TCR one third of magnitude smaller than that of bulk material. This phenomena is called narrow-width effect. Considering the fundamental importance of the material properties of thermistor, the detailed study of the narrow-width effect on TCR and resistivity, and optimization of Pt and Ti thermistors in uncooled antenna-coupled THz microbolometer fabrication are studied in the current report.

2. Experimental

The microbolometer consists of an integrated heater-thermistor and half-wave dipole antenna to detect terahertz wave, designed for 1 THz [15,16]. For the current work test devices without the antenna similar to antenna-coupled microbolometers were fabricated and their characteristics were evaluated at room temperature. The width of the Ti thermistor is made as narrow as 0.1-0.2 μm by electron beam lithography. The microbolometer fabricated this time does not have the gold (Au) antenna, however consists of Ti heater, silicon dioxide (SiO_2)/ nitride (SiN_x) interlayer and Pt or Ti thermistor on SiO_2/SiN_x substrate. The

detailed process steps including electron beam lithography for nanostructures and fabrication of the Ti thin-film thermistor and heater, are discussed elsewhere [14,19,21,22]. The field emission scanning electron micrographs (FE-SEM) are taken on analytical FE-SEM (JEOL JSM-7001F). The electron backscatter diffraction (EBSD) was taken with Bruker's QUANTAX EBSD analysis system supported by the ESPRIT 2 software. In-situ vertically adjustable e^-Flash^{FS} detector used for fast acquisition [630 patterns/s (4 × 4 binning) or 945 patterns/s (8 × 8 binning)]. For an EBSD measurement a flat/polished crystalline specimen is placed in the SEM chamber at a highly tilted angle (~70° from horizontal) towards the diffraction camera, to increase the contrast in the resultant electron backscatter diffraction pattern. The electrical measurements for the nanodevices were done with a low temperature prober equipped with 4156C precision semiconductor parameter analyzer by Agilent. For the measurement of TCR, the slope of resistance vs. temperature graph for five different temperatures from 300K to 240K were used. The responsivity of the fabricated microbolometers is measured by applying AC electrical power up to 2 μW at 10 Hz. Thermistor output was detected by lock-in amplifier under the maximum bias current of 100 μA for Ti and 1000 μA for Pt thermistor.

3. Results and Discussion

Fig. 1 shows the devices fabricated for measurement of the width effect on the thermistor, which includes straight wire structures with variable widths. For the current design of microbolometer, the width for thermistor could be about .01 μm or .02 μm.

Test devices are fabricated with straight devices with design width (DW) = .05 to 5 μm, with fixed length (100 μm) and height (.05 μm). Fig. 1(a) shows optical microscope (OM) image of straight wire thermistor of test devices with DW= 0.5 and 0.6 μm, and further the amplified top-view of the thermistors by FE-SEM with fig. 1(b) DW = 0.5, and fig. 1(c) 0.6 μm is shown. It is observed from FE-SEM that the top width of the thermistors are lower than bottom, shown as the demarcation lines [fig. 1(c)]. This may be caused to the shadow effect in the vacuum evaporation, the width of the top and bottom of the thermistor is different. An average measured (AMW) with is defined as the average of the experimentally measured inner width (MIW) and measured outer width (MOW). Fig. 1 (e) shows variation of the average measured value of width (AMW) for the inner and outer demarcation lines (corresponding to the top and bottom width of the thermistor), with design width (DW) for two different substrates (SiO_2 and SiN_X) and Pt and Ti. The differences between the DW and the AMW width is noticeable, for the region of our interest (DW=1 μm-0.1 μm). Hence, for reliability, TCR and resistivity, have been analyzed with average measured width (AMW), instead of DW. It is also noticeable that that the data at DW= .05 μm is deflected

from the trend of the graph and hence may not be reliable either and hence has been eliminated from discussion.

Fig. 2 shows the TCR and resistivity (ρ) with the variation for (a) Pt and (b) Ti thermistors for two different substrates (SiO_2 and SiN_X) and straight structures with the variation of the AMW (DW = 0.05 -5 μm) of the thermistors, with length L= 100 μm, height H=.05 μm. the correlation between increased resistivity and reduced TCR is observed commonly for both the metal and different substrates with reduction of width. The TCR and resistivity, could be well fitted with empirical formulae for [fig. 2(a)] Pt and [fig. 2(b)] Ti devices, which hold well for on both substrates. Table I. gives the variation of TCR and resistivity based on the empirical equations for two extreme values of experimental AMW = 100 nm and 5000 nm to find the factor of narrow-width effect in these two materials for different substrates. It is found that the narrow-width effect in the devices of (i) Pt (on SiO_2/Si): TCR reduction to 58%, ρ increase by a factor of 2; (ii) Pt (on SiN_x/SiO_2/Si): TCR reduction to 58%, ρ increase by a factor of 1.8. Also the narrow-width effect in the devices of (iii) Ti (on SiO_2/Si): TCR reduction to 40%, ρ increase by a factor of 3; (iv) Ti (on SiN_x/SiO_2/Si): TCR reduction to 44%, ρ increase by a factor of 3.5. From these results, it is evident that the narrow-width effect for TCR is far higher for Pt than for Ti, whereas the narrow-width effect for resistivity for Pt is lower than Ti. However, negligible substrate effect on TCR and resistivity can be observed. Though SiN_x on SiO_2 as substrate has the advantage of high temperature applications and may be preferable substrate for further investigations.

Considering the importance of TCR, the narrow-width effects on the TCR and resistivity for Ti thermistor is further investigated for correlation with grain size and grain orientation of the metals by EBSD, which is an SEM-based technique applied to materials microstructural characterization to study any crystalline or polycrystalline material with high lateral resolution. This involves understanding the microstructures, crystal orientation and phase of materials, revealing texture, defects, grain morphology and deformation. For further understanding the EBSD, pole figures are used to plot 3D orientation information in two dimensions such as on a paper sheet or a computer screen. They are suited for showing the orientations of specific crystallographic planes and directions within a sample (i.e. for plotting the texture) and, as such, are invaluable for EBSD. Fig. 3. shows the EBSD results for (a) large-area Ti film (150 × 150 μm) and (b) Ti nanowire with DW ~ 100 nm for a comparative study. In fig. 3. (a) and (b) may be useful to have an idea about the variation of the materials property with the change of width. In terms of (i) phase: from the phase map, it is clear that Ti hexagonal phase is far higher (~90%) than that of Ti cubic phase, however they remain the same in ratio for (a) and (b); (ii) grain distribution: from grain distribution map, the

different colours mark the grain boundaries to separately define one grain from another grain. Here the colours do not signify any particular gain size or size range in the map. However, apparently from the images (a) and (b), it may be assumed that the size of the defined grain boundaries are large for large area

Ti film; (iii) grain distribution: from the grain distribution statistics from the grain distribution map, it is observed that the number of grain in large area Ti film is far lower (2434) with respect to Ti nanowire (7412) whereas the average grain size as detected by EBSD is higher for Ti film (39.2 nm) than Ti nanowire (31.9), which is a notable observation. Though it is best to correlate the grain size results with some standard characterization methods like transmission electron microscopy (TEM) or X-ray diffraction or micro-Raman spectra. However, it is to be noted that our efforts for testing of grain size with X-ray or micro-Raman failed, largely due to the area of our interest is only about 100-5000 nm of width of a nanowire and it is not possible to focus in these without FE-SEM. TEM is a destructive process and have not been tried with the devices yet. A comprehensive study on the grain size with the variation of the width may be done in an advanced level of the current study. From these EBSD results though we can still conclude: whereas there is no remarkable variation in terms of phase map, phase ratio, local diffraction patterns, grain distribution map; there is difference in grain statistics that is the grain size for Ti films is higher than that of Ti nanowire. Fig. 4. shows the EBSD results with 2D pole figures and 3D pole figures (diffraction spheres) with different viewing angles for large-area Ti film (150 × 150 μm) and Ti nanowire with DW= 100 nm. Though the results are not very conclusive for the study of the grain or plane orientations of the crystals, which may be due to randomness of the grains that no fixed or single orientation is available. This may be due to the room-temperature growth of the thin films from which the wires are made by lift-off process. A high-temperature growth form metal evaporation may give a highly orientated metal film. Here we can only conclude that no noticeable variation is observed for 2D and 3D pole figures with different viewing angles for the large area Ti film and Ti nanowire of DW=100 nm.

It may be concluded that the crystal orientation largely depend on deposition temperature of the film (room temperature electron-beam evaporation, in this cases) if other parameters are fixed. That is, the narrow-width effects in electrical properties are not linked with crystal orientation. Rather from figs. 3 and 4, it may be observed that reduced TCR and enhanced resistivity is correlated with the reduced grain size, in addition to the conventional size effect by the increased surface scattering. In order to understand the mechanism of the resistivity-TCR correlation, detailed material studies are necessary, which may lead to the improved performance of the metal-resistor-based bolometers. The optimum value for TCR and resistivity at thermistor DW= 0.1 μm (i.e. 100 nm) and 0.2 μm are further used, considering the design

requirement for the fabrication of uncooled antenna-coupled terahertz microbolometer test devices and are investigated. Here two sets of identical devices are fabricated similar to uncooled antenna-coupled terahertz microbolometer but without the antenna for the measurement of the electrical responsivity on different bias currents. Microbolometer devices with identical dimensions are made separately on the same chip for the measurement optical responsivity, and are under investigation. However, we can expect that the optical responsivity is reflected to electrical responsivity and hence the current report deals with the electrical result correlating the device performance with material aspects. Fig. 5. shows the layout design, with the realization of the design on SiN_x substrate with OM image and enlarged FE-SEM view showing the heater and straight structured thermistor suspended above the cavity in silicon substrate for testing devices with thermistor DW= 0.1 and 0.2 μm, heater DW= 2.1 μm, and common length of heater and thermistor L= 25 μm to measure the electrical responsivity on different bias currents.

On one of the most important figure of merit to consider when designing and optimizing microbolometer performance is responsivity (R_V). Considering the signal voltages can be quite low for these devices, microbolometer with higher responsivities could reduce the amplification requirements in receiver systems. The bolometer's electrical responsivity is the measure of thermistor output V_{out} with respect to input power applied to the heater. Responsivity (R_V) is defined as follows:

$$R_V = I_b \frac{dR_D}{dP_{in}} \; in \frac{Volts}{Watt} \qquad eq\ (1)$$

where I_b is the DC bias current through the thermistor, and $\frac{dR_D}{dP_{in}}$ is the change in resistance of the detector due to power absorption in the load. For resistive type microbolometers, the load element also acts as the detector. It is evident that the responsivity can be optimized by maximizing the product of I_b and $\frac{dR_D}{dP_{in}}$.

The analysis could further be extended to:

$$R_V = I_b \frac{dR_D}{dP_{in}} \; in \frac{Volts}{Watt} = K\, I_b\, R_{th} \alpha_{th} \quad eq\ (2)$$

where I_b is the DC bias current through the thermistor with resistance R_{th} and TCR $=\alpha_{th}$ and K is a proportionality constant, which also depends on materials properties. The detailed theoretical calculations related to the above may be found in our previous work [19]. Considering these in physical constants, the role of the material properties of the thermistor and heater becomes much clearer. Hence from eq. (1,2) it is evident the slope of the input power vs. output voltage of the bolometer gives the electrical responsivity. It is also clear the responsivity is proportional to the (i) bias current (I_b) applied to the thermistor, (ii) thermistor resistance and (iii) thermistor TCR.

Considering the heating in a thermistor suspended in air, the effect of high current is quite sharp and may

create undesirable and irreversible elongation damage to the device. An interesting experiment to extract the maximum power that Ti microbolometer element can sustain without performance degradation is made by Saxena, *et al.* [23]. The normalized resistance linearly increases with the square of the current and amount of the resistance change increases with resistors length, have been observed and discussed analytically by Zhang *et al*. [24] for an isolated wire. Our electrothermal circuit simulation further incorporates heat loss caused by the leads of thermistor and the heater voltage terminal [19] to establish the dependence of microbolometer's responsivity on sizes and material characteristics of the thermistor and heater.

In our current measurements, we have consistently used the maximum allowable current/voltage across the thermistor (which heats up and the change of resistance due to heating in the thermistor) to ~3 % rise of resistance to that of room-temperature resistance (R_0). Hence, it is likely that the device may handle far higher bias current without breaking, and show a higher responsivity. However our current intentions are to have a comparative understanding for thermistor DW= 0.1 and 0.2 μm for Pt and Ti metal, not by flowing higher excessive current, and to establish the benefit from either material linking its TCR and resistivity [14]. For the microbolometer fabrication the resistance of the thermistor, rather than resistivity, is an important parameter considering that the dimensions of the thermistor and heater are limited by the design and size of the entire detector including antenna. For the miniaturization of the device, either a higher resistive material is to be used or other design aspects are to be considered. Allowable length for thermistor could be availed by more complex layout pattern of the thermistor, e.g. meander shape, with longer effective length even with the miniaturized device, resulting in enhanced electrical responsivity. However, the most vital aspect of microbolometer fabrication is the TCR. The

responsivity is proportional to the TCR and NEP is inversely proportional to the TCR. However, having a thinner thermistor reduces the TCR while increasing the resistivity, and hence a trade-off may arise. In the current design of the thermistor, TCR suffers reduction of almost about 1/3rd of the bulk value.

Fig. 6. gives voltage input-output response for heater for Pt and Ti microbolometer devices with thermistor width DW= 0.2 μm and 0.1 μm and fixed length along with electrical responsivity at maximum allowable bias currents to thermistor at a frequency= 10Hz. It is found that (i) the device with DW= 0.1 μm of Ti thermistor has ~ 1.5 time higher electrical responsivity (376 V/W) at maximum allowable current than that with DW= 0.2 μm (254 V/W); and which is also ~11 times higher than device with DW= 0.1 μm of Pt thermistor. (ii) The device with DW= 0.1 μm of thermistor has higher value of electrical responsivity at reasonably lower bias current than that of device with DW= 0.2 μm of thermistor. (iii) The same value of resistance increase due to temperature rise (3% of room-temperature resistance) took almost 10 times

higher bias current in Pt devices than Ti devices even with the same DW of thermistor. From table I. it may be concluded, at a low DW = 0.1 and 0.2 μm, the TCR difference is not remarkable in Pt and Ti. However, the resistivity of Ti is about 4.5 times higher than that of Ti nanowire of DW = 0.1 μm, which could be the cause of higher responsivity for Ti devices. The interesting observation is the higher responsivity of both Pt and Ti devices with lower (DW=0.1 μm) of thermistor than higher (DW=0.2 μm) where the TCR is lower but resistivity is higher. However, from eq (2) the relationship of TCR and resistivity with electrical responsivity may not be very straight forward and a detailed analytical model is presented in our previous work [19].

Not many comparative studies are available for Pt or Ti microbolometers to assess the current devices. Whereas the reports deal with VO_2 or VO_X [13,25-27], even gives higher responsivity but is expensive, i.e. less abundant as natural resource, and has some difficulty in integration with standard or available device manufacturing technology. However a few important results may be noted with absorber type Ti: (i) responsivity =1600 V/W with 256 × 256 array size [28] (ii) responsivity =30 V/W with 16 × 16 array size [23] and with half-wave antenna coupled Ti: (iii) responsivity =90 V/W with unit device [16]. The report by Saxena, *et al.* [23] is comparable, which presents a meander kind of structure with DW=2 μm (about 10/20 times higher than the current work) but with a responsivity of 30 V/W. Though exact comparison is not possible due to difference in structure and measurement conditions, the current devices with Ti stand out in terms of performance of the unit device and offer better application prospects considering the compatibility and ease of fabrication with currently available technologies and scope of further miniaturization. However, the main highlight of current work, a detailed investigation on the narrow-width effect of TCR for Ti or any metallic nanoscale wire, to our knowledge, is still unavailable.

To understand the exact mechanism for the variation of TCR or resistivity with width in a lower dimension, several sources of electron scattering are to be considered; e.g. scattering arising from interactions between electrons and phonons, between electrons and defects or impurities, and between electrons and interfaces including grain boundaries and free surfaces, along with surface scattering and grain boundary scattering [29]. Studies have demonstrated [29-32], the thickness dependence of the electrical resistivity of thin metal films. This could be due to electron scattering at grain boundaries compared to surface scattering and the impact of grain sizes as suggested based on standard resistivity models [29,30]. The increase of resistivity with lowering of width is proposed based on the electron mean free path, and may be understood from the fact that the resistivity for Cu wires increase faster with reduction of width than Al, because Cu has longer electron mean free path than Al [33]. It is also found that the grain size increases with the film thickness for platinum films, and saturates for large thickness [29,34]. This result may be comparable to the current

scenario of Ti films with increased width increases grain size and reduces number of grains as seen by EBSD. Thin Ti films are analyzed accounting for electron scattering at both film and grain boundary surfaces and lowering of resistivity is shown to correlate directly with an increase in grain size and hence increase of width and saturates at a certain value of grain size [35], with ρ reaching the bulk value of the material. Interestingly, narrow-width effect can be observed in a single-crystal wire with no grain also. Hence though grain size effect is important, primary effect comes from the reduction of the width and thickness. However, though there are some interesting studies available for metal interconnects on the width effect of resistivity, a comprehensive study and understanding on TCR and ρ for Ti is not available specially for the narrow-width effects to be considered for nanodevices where the grain size is <100 nm. The correlation between TCR and resistivity could also be interesting and hence, currently under investigation.

The intentions of the current report is to highlight and minimize the narrow width effect in thin metal interconnects by studying how it affects the TCR and resistivity of the metal thermistor and hence the final performance of the detectors in terms of electrical responsivity. A higher TCR is good for the detector performance but that is compromised in lower dimensional devices in efforts to miniaturize the detectors. Here the TCR falls drastically from DW= 5 μm to DW= 0.2 or and further to 0.1 μm for both the thermistor metal candidate. Still we found DW=0.1 μm is better in terms of electrical responsivity than that of DW=0.2 μm. Hence the effect of lowering of TCR is minimized due to higher resistivity in DW= 0.1 than that of DW=0.2 μm. In the current report as the focus has been emphasized mainly on the effect of width change (TCR and resistivity variation) and how it is going to impact the electrical responsivity of the detectors, a detail investigation on the scaling of electrical noise, though is important, but was not and detailed noise analysis with respect to the change of width is underway currently. However the scaling trend in terms of length of the electrical responsivity and cutoff frequency of the integrated thermistor and heater for microbolomter, was studied explicitly in our previous report [19, 21], and may be useful for a comprehensive understanding. The responsivity was found to increase upon length increase, if the width and thickness of the heater-thermistor are kept the same. To miniaturize the device still have a higher responsivity a meander structure may be useful. Though the aim for final application of these thermistors is in the terahertz antenna-coupled microbolometers, however for this report the focus has been emphasized mainly on the effect of width change (TCR and resistivity variation) and how it is going to impact the electrical responsivity of the detectors. It is to be noted that we can expect the electrical responsivity result for microbolometers are reflected to the optical (THz wave) responsivity of the antenna−coupled microbolomters. Hence the current report does not include the detector's optical perforce

in THz wave. The gold electrodes here, are not acting as antennas and do not contribute significantly to the electrical measurements because of the four probe measurement method used. A detail study on the fabrication and electrical and optical performance of uncooled antenna-coupled terahertz microbolometer arrays with fine line meander structure Ti/Pt thermistors with DW= 0.1 μm and 0.2 μm is under investigation currently, with the insights provided in the current report.

4. Conclusions

Considering the importance of TCR, the narrow-width effect in the TCR and resistivity for Pt and Ti thermistor with various design width (DW)= 0.1~5 μm on two different substrates (SiO_2/Si and SiN_X/SiO_2/Si) are investigated. Increased resistivity and reduced TCR of the devices with the decreased line width, is observed commonly for both metal and fitted with empirical formulae, which hold well for different substrates. It is evident from the EBSD results showing reduced average grain size from Ti film to Ti nanowire (DW=0.1 μm), that the reduced TCR is not dependent on crystal orientation or phase variation of material but can be correlated with reduced grain size due to reduction of width. The optimum value considering design requirement, thermistor of DW =0.1 μm and 0.2 μm is used for the fabrication of microbolometer. It is found that the device with DW= 0.1 μm of Ti thermistor has ~ 1.5 time higher electrical responsivity (376 V/W) at maximum allowable current than that with DW= 0.2 μm (254 V/W), and the former is also ~11 times higher than device with DW= 0.1 μm of Pt thermistor. Also the same ratio of resistance increase due to temperature rise (3% of room-temperature resistance) requires almost 10 times higher bias current in Pt devices than Ti devices with the same DW of thermistor. In order to understand the mechanism of the resistivity-TCR correlation, detailed material studies are necessary, which may lead to the improved performance of the metal-resistor-based bolometers. The results in current report lead to the detailed understanding of the width effect of TCR for Ti in the dimension of nanodevices, to our knowledge, is not available at present. Cause of higher responsively could be higher TCR or resistivity, or a trade-off in both. The optical response with THz source is under investigation currently, but it is reasonably expected to have proportional improvements.

Acknowledgments

This work was supported by JSPS KAKENHI Grant Number 15H03990, the Cooperative Research Project of Research Institute of Electronics, Shizuoka University, and the Cooperative Research Project Program of RIEC, Tohoku University.

References

[1] P. Martyniuk, J. Antoszewski, M. Martyniuk, L. Faraone, A. Rogalski1, New concepts in infrared photodetector designs, Appl. Phys. Rev. **1**, (2014) 041102.

[2] R.M. Woodward, B.E. Cole, V.P. Wallace, R.J. Pye, D.D. Arnone, E.H. Linfield, M. Pepper, Terahertz pulse imaging in reflection geometry of human skin cancer and skin tissue, Phys. Med. Biol. **47**, (2002) 3853.

[3] M. Nagel, P.H. Bolivar, M. Brucherseifer, H. Kurz, A. Bosserhoff, R. Buttner, Integrated THz technology for label-free genetic diagnostics, Appl. Phys. Lett. **80 (1),** (2002) 154.

[4] N. Karpowicz, H. Zhong, C. Zhang, K.I Lin, J.S. Hwang, J. Xu, X.C. Zhang, Compact continuous-wave subterahertz system for inspection applications, Appl. Phys. Lett. **86 (5)**, (2005) 054105.

[5] K. Yamamoto, M. Yamaguchi, F. Miyamaru, M. Tani, M. Hangyo, Non-invasive inspection of c-4 explosive in mails by terahertz time-domain spectroscopy, J. Appl. Phys. **43 (3B)**, (2004) L414.

[6] K. Kawase, Y. Ogawa, Y. Watanabe, H. Inoue, Non-destructive terahertz imaging of illicit drugs using spectral fingerprints, Opt. Express 11 (20), (2003) 2549.

[7] C. Joerdens, M. Koch, Detection of foreign bodies in chocolate with pulsed terahertz spectroscopy, Opt. Eng. **47 (3)**, (2008) 037003.

[8] M. Tonouchi , Cutting-edge terahertz technology, Nat. Photonics **1**, (2007) 97.

[9] P.H. Siegel, Terahertz technology, IEEE Trans. Microwave Theory Tech. **50**, (2002) 910.

[10] A. Rogalski, F. Sizov, Terahertz detectors and focal plane arrays, Opt. Elec. Rev. **19**, (2011) 346.

[11] M.V.S. Ramakrishna, G. Karunasiri, P. Neuzil, U. Sridhar, W.J. Zeng, Highly sensitive infrared temperature sensor using self-heating compensated microbolometers, Sens. Actuators A **79,** (2000) 122.

[12] F. Niklau, C. Vieider ,H. Jakobsen, in MEMS/MOEMS Technologies and Applications III, edited by J.C. Chiao, X. Chen, Z. Zhou, X. Li, Proc. of SPIE 6836, 68360D, (2007) pp. 1-15.

[13] S. Chen, H. Ma, S. Xiang, X. Yi, Fabrication and performance of microbolometer arrays based on nanostructured vanadium oxide thin films, Smart Mater. Struct. **16,** (2007) 696.

[14] A. Tiwari, H. Satoh, M. Aoki, M. Takeda, N. Hiromoto, H. Inokawa, Analysis of Microbolometer Characteristics for Antenna-Coupled Terahertz Detectors, Asian J. Chem. **25,** (2013) S358.

[15] N. Hiromoto, A. Tiwari, M. Aoki, H. Satoh, M. Takeda, H. Inokawa, Room-temperature THz antenna-coupled microbolometer with a Joule-heating resistor at the center of a half-wave antenna, 39th International Conference on Infrared, Millimeter, and Terahertz waves (IRMMW-THz), Tucson, AZ, USA , 14-19 Sept. 2014 (DOI: 10.1109/IRMMW-THz.2014.6956173).

[16] M. Aoki, M. Takeda and N. Hiromoto, Proc. Int. Conf. Global Research and Education (Inter

Academia), 2A-3 (Budapest, Hungary, August 27-30, 2012), pp. 65.

[17] Y.L. Cheng, B.J. Wei, F.H. Shih, Y.L. Wang, Stability and Reliability of Ti/TiN as a Thin Film Resistor, ECS J. Solid State Sci. Techn. **2,** (2013) Q12.

[18] A. Tanaka, S. Matsumoto, N. Tsukamoto, S. Itoh, K. Chiba, T. Endoh, A. Nakazato, K. Okuyama, Y. Kumazawa, M. Hijikawa, H. Gotoh, T. Tanaka, N. Teranishi, Infrared focal plane array incorporating silicon IC process compatible bolometer, IEEE Trans. Electron Devices **43,** (1996) 1844.

[19] A. Tiwari, H. Satoh, M. Aoki, M. Takeda, N. Hiromoto, H. Inokawa, Fabrication and analytical modeling of integrated heater and thermistor for antenna-coupled bolometers, Sensors and Actuators A: Physical **222**, (2014) 160.

[20] Jason Lewis, PhD Dissertation on Far-Infrared and Sub-Millimeter Microbolometer Detectors, The University of Texas at Austin, 1994, Chapter: Factors Affecting Microbolometer Responsivity, http://www.weewave.mer.utexas.edu/MED_files/MED_research/microbolometers/microblmtr_anlys/bolo_respnsvty.html

[21] A. Tiwari, H. Satoh, M. Aoki, M. Takeda, N. Hiromoto, H. Inokawa, THz Antenna-Coupled Microbolometer with 0.1-μm-wide Titanium Thermistor, Int. J. ChemTech Res. **7,** (2014-2015) 1019.

[22] A. Banerjee, H. Satoh, A. Tiwari, C. Apriono, E. T. Rahardjo, N. Hiromoto and H. Inokawa, Width dependence of platinum and titanium thermistor characteristics for application in room-temperature antenna-coupled terahertz microbolometer, Jpn. J. Appl. Phys. **56**, (2017), 04CC07.

[23] R.S. Saxena, R.K. Bhan. P.S. Rana, A.K. Vishwakarma. A. Aggarwal, K. Khurana, S. Gupta, Study of performance degradation in Titanium microbolometer IR detectors due to elevated heating, Infrared Physics & Technology, **54 (4)**, (2011) 343-352.

[24] S. Zhang, Y. Yang, S.M. Sadeghipour, M. Asheghi, Thermal Characterization of the 144 nm GMR Layer using Microfabricated Suspended Structures, Proceedings of ASME Summer Heat Transfer Conference, Las Vegas, Nevada, USA, July 21-23 (2003) HT 2003-47270.

[25] C. Chen, X. Yi, X. Zhao, B. Xiong, Characterizations of VO_2-based uncooled microbolometer linear array, Sensors and Actuators A. **90**, (2001) 212-214.

[26] H. Wang, X. Yi, G. Huang, J. Xiao, X. Li, S. Chen, IR microbolometer with self-supporting structure operating at room temperature, Infra. Phys. Technol. **45**, (2004) 53-57.

[27] C. Chen, X. Yi, J. Zhang, X. Zhao, Linear uncooled microbolometer array based on VO_x thin films, Infra. Phys. Technol. **42**, (2001) 87-90.

[28] H. K. Lee, J. B. Yoon, E. Yoon, S. Baek Ju, Y. J. Yong, W. Lee, and S. Gook Kim, A high fill-factor infrared bolometer using micromachined multilevel electrothermal structures, IEEE Trans. Electron

Devices **46**, (1999) 1489-1491.

[29] V. Barnat, D. Nagakura, P.I. Wang, T.M. Lu, Real time resistivity measurements during sputter deposition of ultrathin copper films, J. Appl. Phys. **91**, (2002) 1667.

[30] G. Schindler, G. Steinlesberger, M. Traving, M. Engelhardt, Comprehensive study of the resistivity of copper wires with lateral dimensions of 100 nm and smaller, J. Appl. Phys. **97**, (2005) 023706.

[31] Q. Huang, C.M. Lilley, M. Bode, R. Divan, Surface and size effects on the electrical properties of Cu nanowires, J. Appl. Phys. **104**, (2008) 023709.

[32] Y. Kitaoka, T. Tono, S. Yoshimoto, T. Hirahara, S. Hasegawa, T. Ohba, Direct detection of grain boundary scattering in damascene Cu wires by nanoscale four-point probe resistance measurements, Appl. Phys. Lett. **95**, (2009) 052110.

[33] Y. Hanaoka, K. Hinode, K. Takeda, D. Kodama, Increase in Electrical Resistivity of Copper and Aluminum Fine Lines, Mater. Trans. **43(7)** (2002) 1621.

[34] L.L. Melo, A.R. Vaz, M.C. Salvadori, M. Cattani, Grain sizes and surface roughness in platinum and gold thin films, J. Metastable Nanocry. Mater. **623** (2004) 20-21.

[35] M.E. Day, M. Delfino, J.A. Fair, W. Tsai, Correlation of electrical resistivity and grain size in sputtered titanium films, Thin Solid Films **254 (1),** (1995) 285.

Biography

Dr. Amit Banerjee received Ph.D. degree in Semiconductor Technology from Energy Research Unit, Indian Association for the Cultivation of Science (D.S.T., Govt. of India), Kolkata in 2016. In the same year, he joined the Advanced Device Research Division, Research Institute of Electronics, Shizuoka University, National University Corporation, Japan as a Scientific Researcher. Amit has extensively worked on high vacuum plasma CVD reactors, which are heavily used in industrial manufacturing of solar cells, coatings and TFTs. His current work is on Terahertz Technology, including THz devices (sensors and sources) fabrication, materials engineering, and optimization for surveillance, inspection, biomedical and imaging applications.

Dr. Hiroaki Satoh received the B.E. degree from the Muroran Institute of Technology, Hokkaido, Japan, in 1999, and the M.E. and the Ph.D. degrees from Hokkaido University, Hokkaido, in 2001 and 2004, respectively. He was a Research Associate with the University of Tokushima, Tokushima, Japan, from 2004 to 2007. Since 2007, he has been an Assistant Professor with the Research Institute of Electronics, Shizuoka University, Hamamatsu, Japan. His current research interests include the computational electromagnetics, and its application to silicon nanodevices for advanced photonics. Dr. Satoh is a member of the Japan Society of Applied Physics, the Institute of Electronics, Information and Communication Engineers of Japan, and the Institute of Electrical Engineers of Japan.

Yash Sharma, received B.E. and M.E. degrees from SRM University, India and Nanyang Technological University, Singapore, respectively. He is currently a doctoral researcher of Graduate School of Engineering at Shizuoka University and engaged on a study of single photon detectors. His research interests also include terahertz imaging and sensing.

Prof. Norihisa Hiromoto received B.S. and Ph.D. degrees in Physics from Kyoto University in 1978 and 1985. His professional activities since joining Communications Research Laboratory (CRL) in 1984 have included research on detector and laser technologies in terahertz region, an asbestos fiber monitor using optical technique. He was the director of Kansai Advanced Research Center of CRL in 2001 and moved to the Ministry of Internal Affairs and Communications (MIC) as a Senior Planning Officer in 2003. He is presently a professor of Shizuoka University after 2005. He has authored and co-authored more than 60 scientific and technical papers and holds four patents in terahertz an optical technology.

Prof. Hiroshi Inokawa received the Ph.D. degree in electrical engineering from Kyoto University, Kyoto, Japan, in 1985. In the same year, he joined the Atsugi Electrical Communications Laboratories, Nippon Telegraph and Telephone Corporation (NTT), Kanagawa, Japan. Since then, he has been engaged in research and development of scaled-down MOS devices and silicon single-electron devices. In 2006, he became a professor of the Research Institute of Electronics, Shizuoka University, Hamamatsu, Japan, where he has been studying nanodevices for advanced circuits and systems. Prof. Inokawa is a member of the Institute of Electrical and Electronics Engineers, the Japan Society of Applied Physics, the Institute of Electronics, Information and Communication Engineers of Japan, and the Institute of Electrical Engineers of Japan.

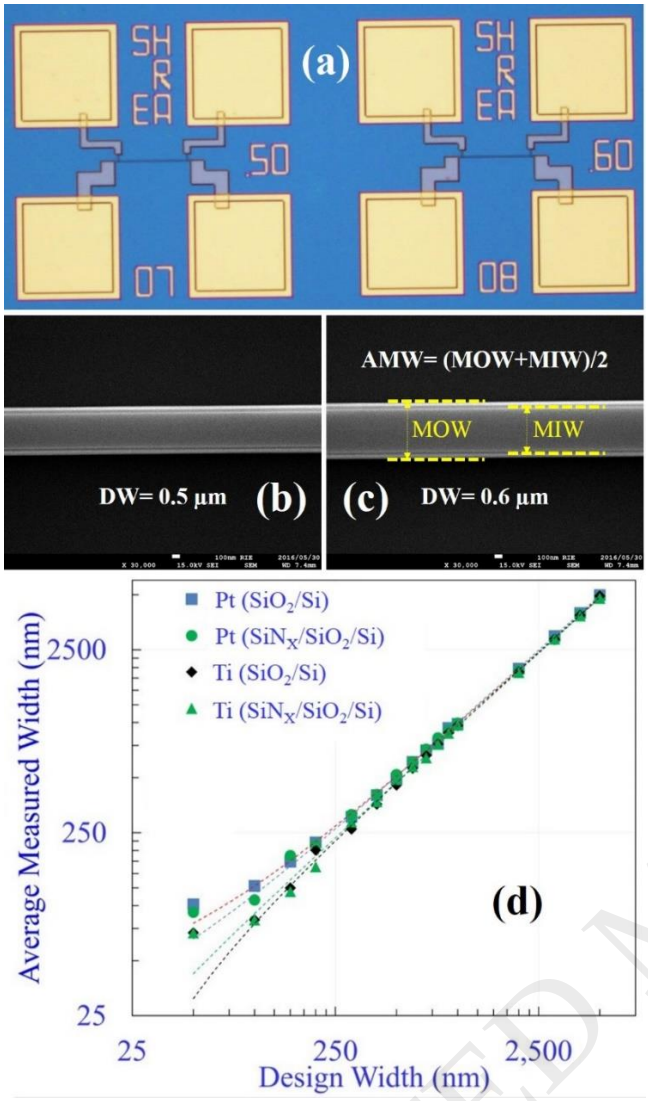

Fig. 1. (a) OM and (b,c) FE-SEM image of Ti straight structured devices fabricated on SiN_x substrate, for measurement of the width effect on the thermistor. (d) Variation of design with (DW) and average measured width (AMW) for two different substrates for Pt and Ti.

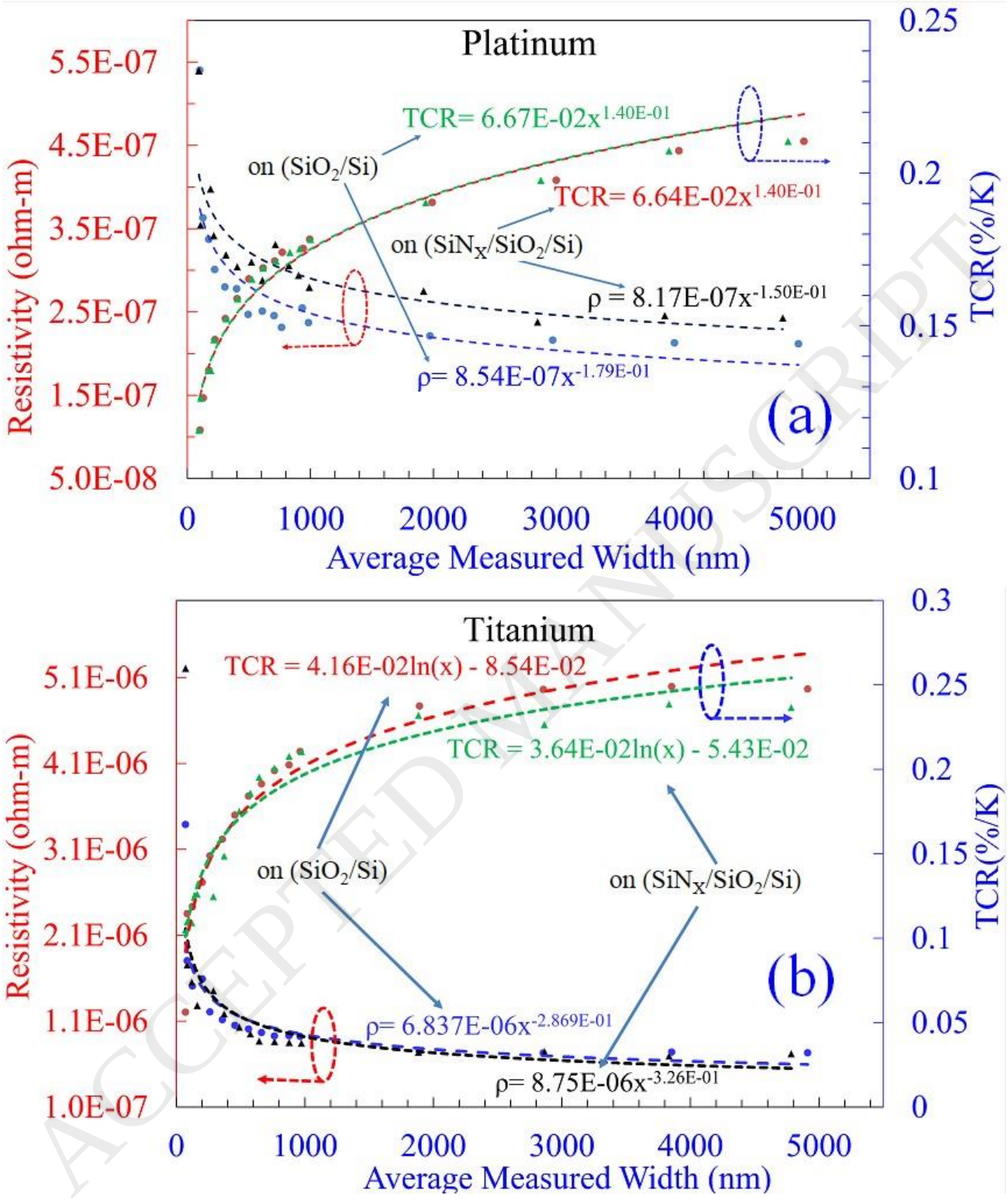

Fig. 2. Temperature coefficient of resistance (TCR) and resistivity (ρ) with the variation of average measured width (AMW) for (a) Pt and (b) Ti thermistor with straight structures on two different substrates.

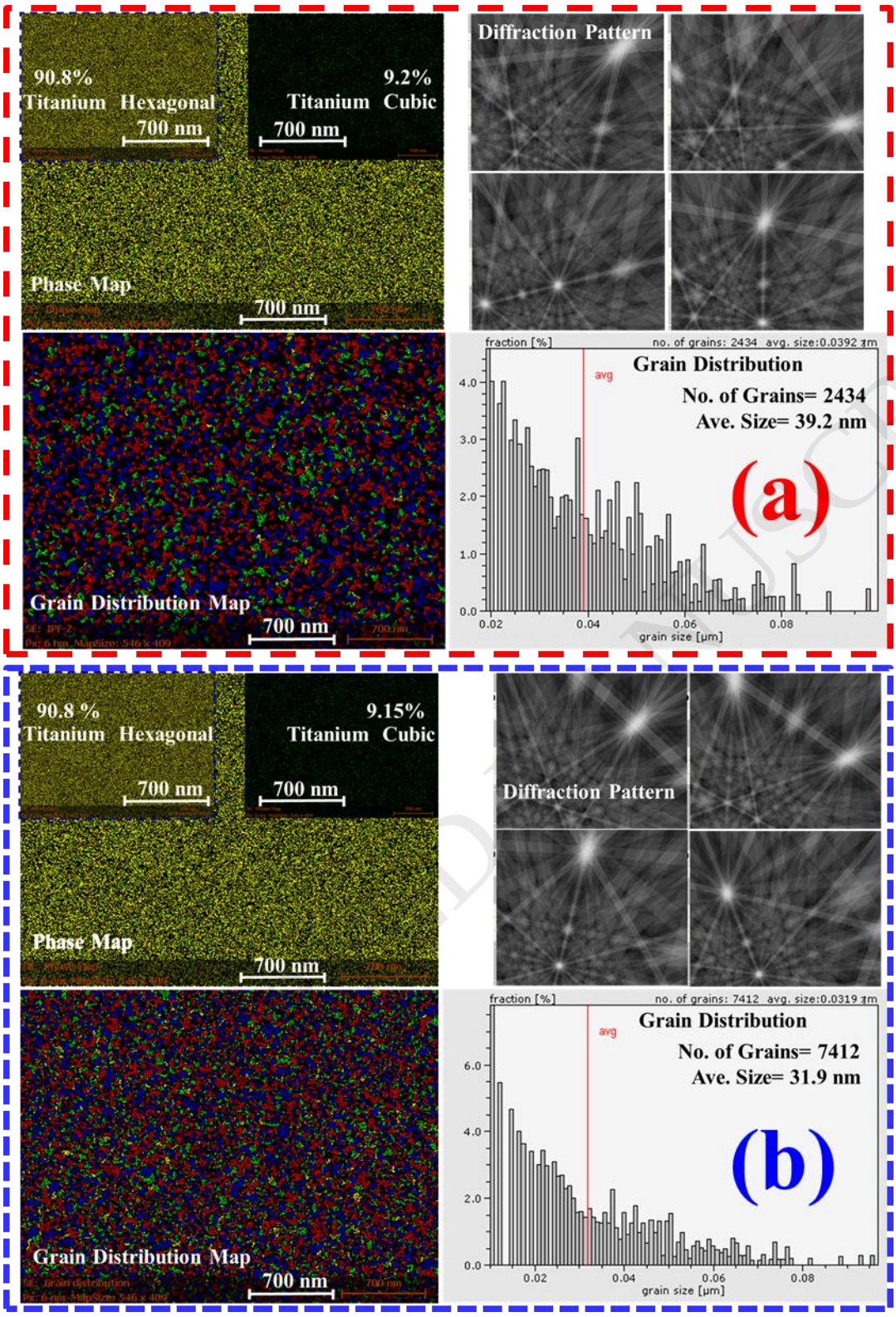

Fig. 3. Electron backscatter diffraction (EBSD) with phase map, phase ratio, local diffraction patterns, grain distribution map and grain statistics for (a) large-area Ti film (150 × 150 µm) and (b) Ti nanowire with design width (DW) = 100 nm.

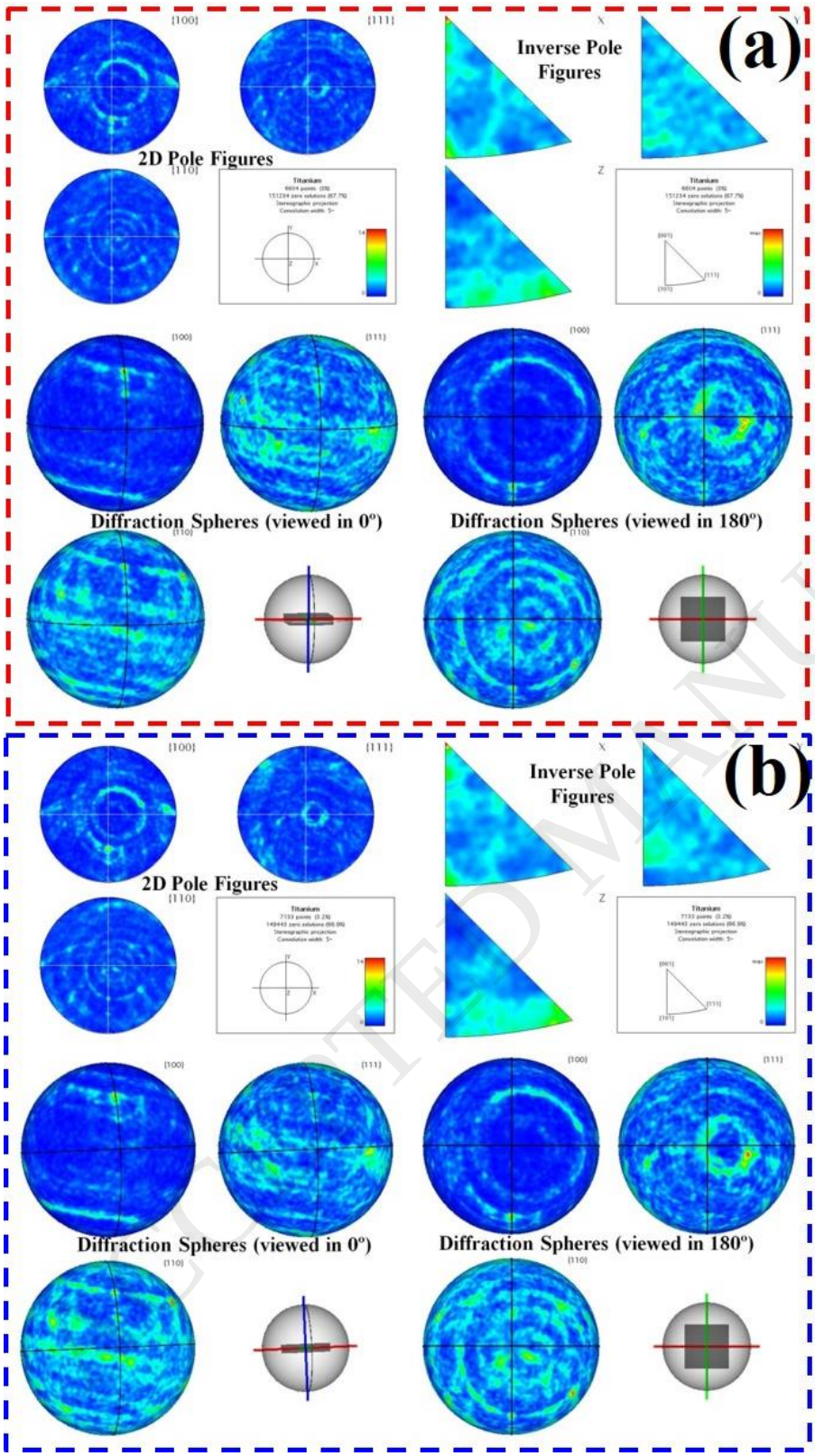

Fig. 4. Electron backscatter diffraction (EBSD) results with 2D pole figures and 3D pole figures (diffraction spheres) with different viewing angles for (a) large-area Ti film (150 × 150 μm) and (b) Ti nanowire with design width (DW) = 100 nm.

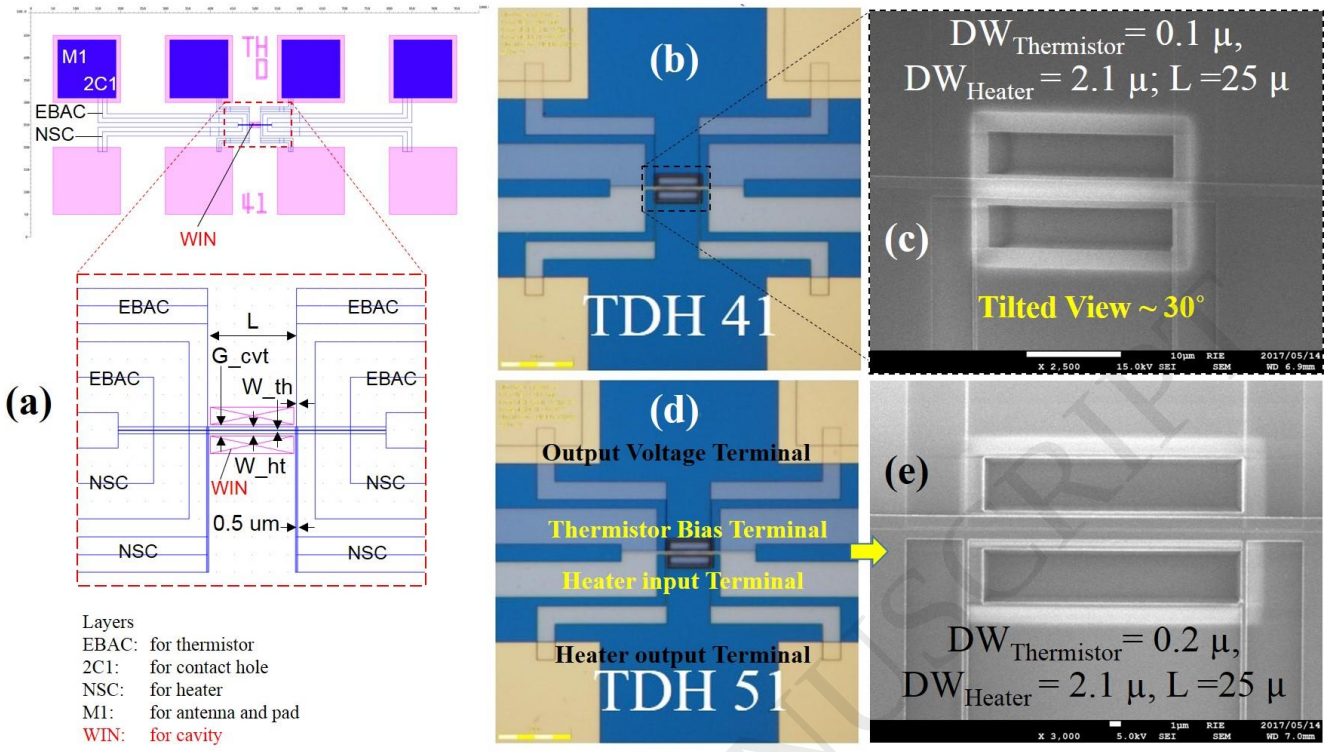

Fig. 5. (a) Layout design and (b) OM image of terahertz microbolometer test device with thermistor DW= 0.1 µm made for the measurement of the electrical responsivity on different bias currents. (c) FE-SEM enlarged view showing the heater and straight structured thermistor suspended on top of the cavity at a tilted view to show the death of the cavity. (d) Electrical input-output terminals used for heater/thermistor of terahertz microbolometer test device with thermistor DW= 0.2 µm and its (e) FE-SEM view. In the final structure of the antenna-coupled bolometer for optical measurement, the heater is directly connected to the dipole antenna, and extra terminals (electrodes) for electrical measurement are eliminated. Thermistor connection is also made by two wires running perpendicular to the antenna direction to eliminate the interference.

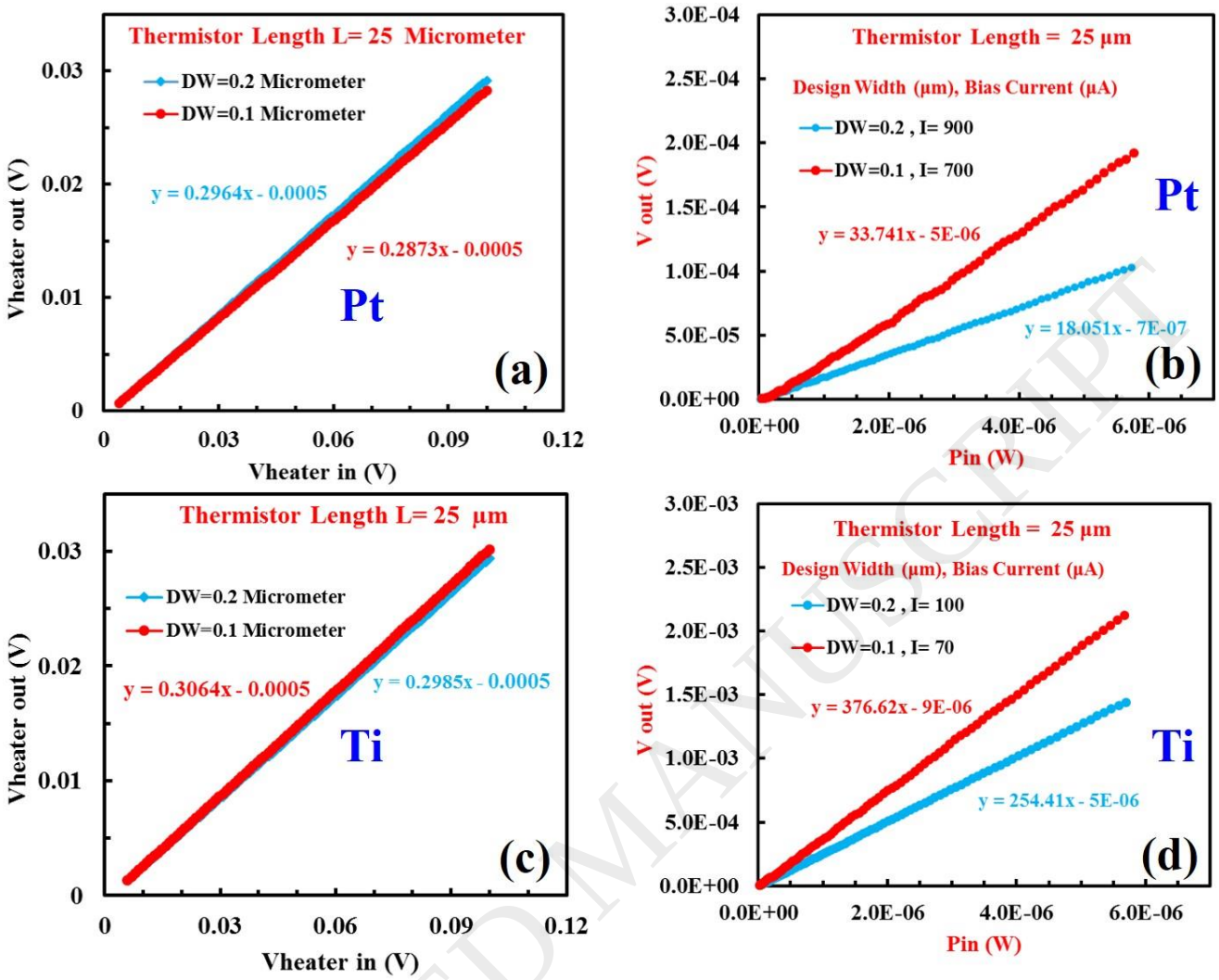

Fig. 6. (a) Voltage input-output response for heater for Pt microbolometer devices with thermistor width DW= 0.2 µm and 0.1 µm and fixed length. (b) Electrical responsivity of Pt microbolometer devices at maximum allowable bias currents to thermistor at a frequency= 10Hz, with thermistor DW= 0.2 µm and 0.1 µm. (c) Voltage input-output response for heater for Ti microbolometer devices with thermistor width DW= 0.2 µm and 0.1 µm and fixed length. (d) Electrical responsivity of Ti microbolometer devices at maximum allowable bias currents to thermistor at a frequency= 10Hz, with thermistor DW= 0.2 µm and 0.1 µm.

Table. I. The variation of TCR and resistivity based on the empirical equations for two extreme values of experimental AMW = 100 nm and 5000 nm for Pt and Ti thermistors on different substrates

Thermistor	**AMW (nm)**	**TCR (%/K)**	**Decrement Factor**	**ρ (Ohm-m)**	**Increment Factor**
Pt (on SiO_2)	5000	0.2198		1.8593E-07	
	100	0.1271	0.578	3.7451E-07	2.01
Pt (on SiN_X)	5000	0.2109		2.2771E-07	
	100	0.1219	0.578	4.0947E-07	1.8
Ti (on SiO_2)	5000	0.2689		5.938E-07	
	100	0.1062	0.395	1.8242E-06	3.07
Ti (on SiN_X)	5000	0.2557		5.447E-07	
	100	0.1133	0.443	1.8242E-06	3.35